



# Functional evidence of distinct electrophile-induced activation states of the ion channel TRPA1

Thomas A. Parks, Parmvir K. Bahia, Thomas E. Taylor-Clark\*

Department of Molecular Pharmacology and Physiology, Morsani College of Medicine, University of South Florida, Tampa, FL, 33612, USA

## ARTICLE INFO

### Keywords:

TRPA1  
Electrophile  
Cysteine  
Activation  
Glutathione

## ABSTRACT

Transient Receptor Potential Ankyrin 1 (TRPA1) is a tetrameric, nonselective cation channel expressed on nociceptive sensory nerves whose activation elicits nocifensive responses (e.g. pain). TRPA1 is activated by electrophiles found in foods and pollution, or produced during inflammation and oxidative stress, via covalent modification of reactive cysteines, but the mechanism underlying electrophilic activation of TRPA1 is poorly understood. Here we studied TRPA1 activation by the irreversible electrophiles iodoacetamide and N-ethylmaleimide (NEM) following transient expression in HEK293 cells. We found that in  $Ca^{2+}$  imaging studies C621 is critical for electrophile-induced TRPA1 activation, but the role of C665 in TRPA1 activation is dependent on the size of the electrophile. We identified slower TRPA1 activation in whole-cell recordings compared to studies with intact cells, which is rescued by pipette solution supplementation with the antioxidant glutathione. Single-channel recordings identified two distinct electrophilic-induced TRPA1 activation phases: a partial activation that, in some channels, switched to full activation with continued electrophile exposure. Full activation but not the initial activation was regulated by C665. Fitting of open time distributions suggests that full activation correlated with an additional (and long) exponential component, thus suggesting the phases are manifestations of distinct activation states. Our results suggest that distinct NEM-induced TRPA1 activation states are evoked by sequential modification of C621 then C665.

## 1. Introduction

Transient Receptor Potential Ankyrin 1 (TRPA1) is a tetrameric, nonselective cation channel that is expressed in a subset of nociceptive sensory neurons [1], whose activation evokes pain, nocifensive reflexes and neurogenic inflammation [2–6]. TRPA1 is activated by a diverse group of endogenous mediators (derived mainly from oxidative stress) and exogenous irritants, many of which are electrophilic [2,7–11]. Functional assays of TRPA1 mutants have identified some N-terminus cysteines (e.g., C621 and C665) as important for electrophile-evoked activation [12–14]. Biochemical and cryo-EM studies indicate that C621 and, to a lesser extent, C665 are rapidly bound by electrophiles [14–16], suggesting that activation occurs through this process. However, the mechanism underlying TRPA1 activation via electrophilic binding of reactive cysteines is poorly understood.

Here, we performed functional studies of TRPA1 constructs to gain further understanding of how electrophiles activate TRPA1, and in particular the role of C665. Complicating this is the under-appreciated discrepancy in the kinetics of TRPA1 activation in intact cells (e.g.,

calcium imaging studies) and whole-cell recordings [9,17,18]. Here, we found that electrophile-evoked whole-cell currents are limited due to the dialysis of cytosolic glutathione (GSH). Single-channel recordings of electrophile-evoked responses indicate two distinct and sequential phases in TRPA1 activation which are differentially regulated by C665.

## 2. Methods

### 2.1. HEK293 cells and TRPA1 constructs

Full length human TRPA1 (hTRPA1) was subcloned into pcDNA3.1 V5-His-TOPO® (Life Technologies; NY) using primers (Biosynthesis; TX) as described previously [14]. Point mutations were made using site-directed mutagenesis via PCR. hTRPA1 WT and mutant channels were expressed in HEK293 cells (cultured in Dulbecco's modified Eagle's medium supplemented with 10% FBS, 100U/ml penicillin and 100 µg/ml streptomycin) using Lipofectamine 2000 (ThermoFisher).

\* Corresponding author.

E-mail address: [ttaylorclark@usf.edu](mailto:ttaylorclark@usf.edu) (T.E. Taylor-Clark).

## 2.2. $Ca^{2+}$ imaging

HEK 293 cell-covered coverslips were incubated with 4  $\mu$ M Fura-2AM (TEFLabs; TX) for 30–60 min. Coverslips were perfused with HEPES buffer ( $\sim$ 34 °C, composed of (mM): 145 NaCl, 10 HEPES, 5.6 dextrose, 4.7 KCl, 1.2 MgCl<sub>2</sub>, 2.5 CaCl<sub>2</sub>, 4.7 KCl; pH adjusted to 7.4 with NaOH), and equilibrated for 10 min prior to experimentation. Changes in intracellular  $Ca^{2+}$  were monitored using sequential excitation at 340 nm and 380 nm (510 nm emission) using microscopy (C13440–20CU; Hamamatsu; NJ) and Nikon Elements (Nikon; NY). Cells were treated with vehicle (0.1% ethanol), iodoacetamide (IA, 30  $\mu$ M), N-ethylmaleimide (NEM, 30  $\mu$ M, ThermoFisher), Thymol (200  $\mu$ M) or 2APB (200  $\mu$ M). In preliminary studies, all TRPA1 constructs displayed significant responses to the non-electrophilic TRPA1 agonist thymol (compared to non-transfected HEK293), indicating the presence of functional channels. Data is presented as  $\Delta 340/380$  ratio: (R-R<sub>bl</sub>), where R is the ratio at a given timepoint and R<sub>bl</sub> is the mean baseline ratio.

## 2.3. Electrophysiology

Voltage-clamp recordings from hTRPA1-expressing or non-transfected HEK293 cells were performed using whole-cell, perforated or cell-attached single-channel techniques ( $\sim$ 22 °C). Only patches with gigaohm seals were analyzed. Patch pipettes were fabricated from 1.5 mm o.d., 1.1 mm i.d. borosilicate glass (Sutter Instruments; CA) and fire-polished. Currents were recorded and analyzed using a MultiClamp 700B amplifier, Digidata 1440A and pClamp 10 acquisition software (Molecular Devices; CA). Whole-cell recordings used a sampling rate of 100 kHz with a 2 kHz single-pole RC lowpass filter. Whole-cell pipettes (3–9M $\Omega$ ) were filled with solution composed of (mM): 130 CsCl, 1 CaCl<sub>2</sub>, 2 MgCl<sub>2</sub>, 10 HEPES, 10 dextrose, 11 EGTA, and 5 Na-tri-phosphate (to prevent rundown of TRPA1 currents [19]); adjusted to pH 7.2 with NaOH. Pipette [ $Ca^{2+}$ ]<sub>free</sub> was  $\sim$ 25  $\mu$ M, which maximizes TRPA1 currents while limiting channel inactivation [26]. Cells were clamped at 0 mV and 500 ms ramps from  $-70$  mV to  $+70$  mV were applied every second. 5 mM glutathione (GSH) or 5 mM ophthalmic acid (OPT) was added to the pipette buffer in some recordings. Perforated patch was achieved using pipettes (1–5M $\Omega$ ) filled with the same solution as the whole-cell studies, supplemented with 25–50  $\mu$ g/ml gramicidin. In both cases cells were perfused with buffer composed of (mM): 145 NaCl, 10 HEPES, 5.6 dextrose, 4.7 KCl, 1.2 MgCl<sub>2</sub>, 0.01 CaCl<sub>2</sub>, 4.7 KCl; pH adjusted to 7.4. Currents were measured in response to NEM (3–30  $\mu$ M), the reversible electrophilic agonist allyl isothiocyanate (AITC, 30  $\mu$ M) and ruthenium red (RR, 30  $\mu$ M), a TRP pore blocker. 200  $\mu$ M Thymol replaced AITC when 3  $\mu$ M NEM was used. The rate of activation was calculated using current density over time (pA/pS/s). Single-channel recordings used a sampling rate of 20 kHz with a 2 kHz single-pole RC lowpass filter, followed by a post-acquisition 1000 Hz 8-pole Bessel low pass filter. Cell-attached patches used pipettes (7–50M $\Omega$ , coated in Sylgard 184) filled with HEPES buffer composed of (mM): 145 NaCl, 10 HEPES, 5.6 dextrose, 4.7 KCl, 1.2 MgCl<sub>2</sub>, 4.7 KCl, 5 EGTA, 5 Na-tri-phosphate; pH adjusted to 7.4. Cells were perfused with the same HEPES buffer. TRPA1 channels were identified by spontaneous conductances observed in voltage steps ( $-80$  mV to  $+80$  mV). Patches were then held at  $+40$  mV, and currents were observed in response to NEM (30  $\mu$ M, 3 min) then thymol (200  $\mu$ M). Half-amplitude threshold analysis [27] was used to idealize single-channel events using Clampfit. Open and closed dwell times were analyzed as square root of events on a logarithmic histogram [28]. Filter dead time was calculated as  $T_d = 0.179/f_c$  [27]. With  $f_c = 1$  kHz,  $T_d = 179\mu$ s, thus all events  $<400\mu$ s were excluded. Dwell times were fitted to sums of exponential components to determine time constants ( $\tau$ ) [27]. Currents were fitted to a Gaussian function, with the peak corresponding to unitary amplitude. The open probability (NPo) for each channel was determined for 1s bins. NEM-evoked channel activity (NPo) was separated into 3 phases: P1/F1 – no measurable change in spontaneous activity; P2/F2 – the phase

following NPo  $>$  threshold NPo (i.e. 0.02); and (for only some channels) F3 – the phase with sustained ( $>$ 5s) and full activation (NPo $>$ 0.9). In some recordings, two channels were detected in a single patch. Although this did not prevent a qualitative identification of partial vs. full activation or the determination of current amplitude, these channels were omitted from the NPo and dwell time analyses.

## 2.4. Statistical analysis

Data were analyzed using Nikon Elements, GraphPad and Clampfit. A p-value less than 0.05 was considered as significant. A two-way ANOVA was used to analyze the relationships of the rate of change with NEM-evoked responses compared to control in whole-cell and perforated patch clamp. Single-channels with partial and full activation profiles were compared using unpaired analysis. F2 and F3 were compared using paired analysis. Chi-square analysis was used to compare the percentage of single-channels that reached full activation between WT and C665S. All data was expressed as mean  $\pm$  S.E.M. unless otherwise noted.

## 2.5. Chemicals

Unless stated otherwise, all chemicals were purchased from Sigma-Aldrich (St. Louis, MO).

## 3. Results

### 3.1. Mutation of key cysteines inhibit TRPA1-mediated $Ca^{2+}$ fluxes evoked by irreversible electrophiles

We had previously shown that IA-evoked activation of TRPA1 was eliminated in C621A and C665L constructs [14]. Here in  $Ca^{2+}$  imaging studies with HEK293 cells expressing hTRPA1-WT and mutant constructs, we observed a rapid increase in  $Ca^{2+}$  fluxes in response to 30  $\mu$ M NEM in WT- and C641A-expressing cells (Fig. 1A). As expected, C621A and C665L mutants failed to activate with NEM treatment (Fig. 1A). Interestingly, NEM-evoked responses were only partially reduced in the C665S mutant (Fig. 1B and D). Whereas 30  $\mu$ M IA produced no activation of C665S (Fig. 1C and D), which nonetheless responded robustly to the non-electrophile thymol (200  $\mu$ M, mean  $\pm$  S.E.M. thymol response of  $0.19 \pm 0.004$  and  $0.18 \pm 0.003$  for WT and C665S, respectively;  $p > 0.05$ ). Thus, the role of C665 in TRPA1 activation depends on the activating electrophile. We noted that activation of TRPA1-WT by thymol was greatly reduced after NEM treatment (Fig. 1A and B) compared with IA treatment. Importantly, in additional control studies (Fig. 1E) the magnitude and the speed of TRPA1 activation by non-electrophilic agonists thymol (200  $\mu$ M) and 2APB (200  $\mu$ M) were not significantly different between WT and C665S (Fig. 1F and G).

### 3.2. Cell dialysis of GSH reduces NEM-induced TRPA1 activation

Previous whole-cell patch clamp studies [9,17,18] have demonstrated slow electrophile-evoked TRPA1 currents when compared to the rapid TRPA1 activation in  $Ca^{2+}$  imaging studies. Given the possibility that whole-cell studies may be disrupting intracellular TRPA1 regulation, we compared NEM-evoked TRPA1 currents in whole-cell and gramicidin-perforated patches (Fig. 2A). All NEM-evoked TRPA1 currents were inhibited by the TRP blocker ruthenium red. NEM failed to evoke currents in non-transfected HEK293 (mean  $\pm$  S.E.M. response  $0.24 \pm 0.6$  pA/pF,  $n = 4$ , not shown). We found that NEM-evoked TRPA1 activation rate (pA/pF/s) was significantly increased in perforated patches ( $p < 0.05$ ) (Fig. 2B). Linear regression analysis showed no significant relationship between access resistance and TRPA1 currents (data not shown), indicating the reduced responses in whole-cell recordings was not due to differences in access resistance. The data thus indicates that disrupting the membrane prevents full TRPA1 activation

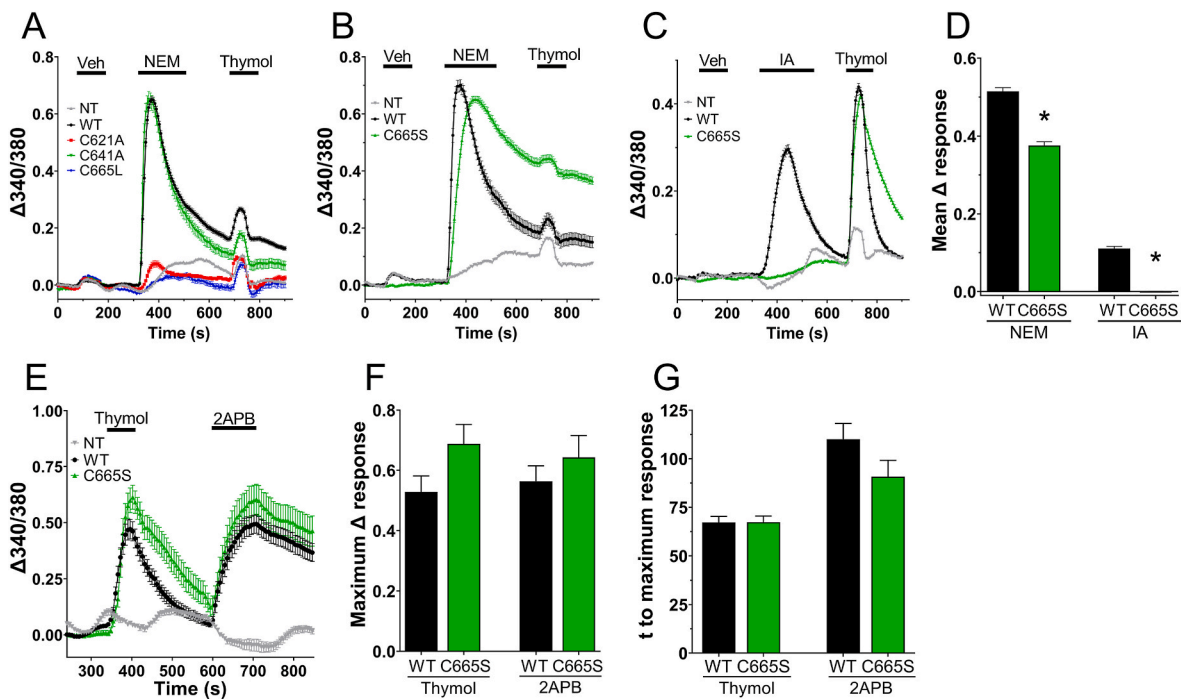


**Fig. 1.** Differential effect of C665S mutation on NEM- and IA-evoked TRPA1-mediated  $\text{Ca}^{2+}$  fluxes. A-C, mean  $\pm$  S.E.M.  $\text{Ca}^{2+}$  responses in non-transfected HEK293 (NT) and HEK293 expressing TRPA1 constructs. A, responses to 0.1% ethanol vehicle (Veh), NEM (30  $\mu\text{M}$ ) and thymol (200  $\mu\text{M}$ ) in NT (n = 237), hTRPA1 wildtype (WT, n = 831), C621A (n = 139), C641A (n = 154) and C665L (n = 80) constructs. B, responses to vehicle (Veh), NEM (30  $\mu\text{M}$ ) and thymol (200  $\mu\text{M}$ ) in NT (n = 79), WT (n = 203) and C665S (n = 642) constructs. C, responses to vehicle, IA (30  $\mu\text{M}$ ) and thymol (200  $\mu\text{M}$ ) in NT (n = 71), WT (n = 388) and C665S (n = 1114) constructs. D, mean  $\pm$  S.E.M.  $\Delta$  NEM-evoked  $\text{Ca}^{2+}$  responses (first 90s) of WT and C665S to NEM and IA. \*,  $p < 0.05$  vs WT. E, responses to thymol (200  $\mu\text{M}$ ) and 2APB (200  $\mu\text{M}$ ) in NT (n = 19), WT (n = 35) and C665S (n = 23) constructs. F, mean  $\pm$  S.E.M.  $\Delta$  responses of WT and C665S to thymol and 2APB. G, mean  $\pm$  S.E.M. time to maximum response of WT and C665S to thymol and 2APB.

by electrophiles, suggesting that an unknown cytosolic component may facilitate rapid TRPA1 activation. Supplementation of the pipette solution with the tripeptide antioxidant GSH (5 mM) in whole-cell recordings caused a significant increase in the NEM-evoked TRPA1 activation rate compared to control recordings ( $p < 0.05$ ) (Fig. 2C and D). However, supplementation with 5 mM OPT, a tripeptide without a cysteine, failed to augment NEM-induced TRPA1 activation (Fig. 2C and D). Although there was a trend for GSH-supplemented currents to exceed a threshold of 5 pA/pF quicker ( $9.4 \pm 1.6\text{s}$ ) than control ( $14.4 \pm 4.5\text{s}$ ,  $p = 0.16$ ) and OPT studies ( $15.7 \pm 3.6\text{s}$ ,  $p = 0.06$ ), this did not reach significance.

### 3.3. Single-channel recordings reveal two distinctive TRPA1 activation phases

We used cell-attached single-channel patch clamp to record gating events during treatment with the irreversible electrophile NEM (30  $\mu\text{M}$ ), thus avoiding membrane disruption. Open probability (NPo) analysis revealed two different NEM-evoked activation profiles: partial activation (Fig. 3A) with transient increases of NPo above threshold levels (P2 phase); and full activation (Fig. 3B), with a sustained ( $>5\text{s}$ ) NPo  $> 0.9$  (F3 phase) following an initial increase in NPo above threshold levels (F2 phase). There were significant differences in the maximum and mean Po evoked by NEM in the full and partial activation profiles ( $p < 0.05$ ) (Fig. 3C), and these were both greater than the almost absent channel activity noted in patches from non-transfected cells (Fig. 3C). There were no differences between the current amplitudes in the partial and full activation profiles (unpaired,  $p > 0.05$ ) and between F2 and F3 phases (paired,  $p > 0.05$ ) (Fig. 3D-F). Fitting of the open time distribution demonstrated 3 exponents in the partial activation profiles (Fig. 3G) and 4 exponents in the full activation profiles (Fig. 3H). There were no differences in the  $\tau$  of the first 3 components between partial

and full activation profiles, but less time was spent during Exp<sub>2</sub> and more time was spent during Exp<sub>4</sub> in full activation profiles ( $p < 0.05$ ) (Fig. 3I and J). Closed times in both partial and full activation profiles had 4 exponents, but the  $\tau$  for Exp<sub>2</sub>, Exp<sub>3</sub> and Exp<sub>4</sub> were significantly shorter in full activation profiles (Fig. 3K-N). We also analyzed the dwell times of F2 and F3 phases separately and found that the exponents for F2 phase (e.g. 3 open time exponents) were not significantly different from the partial activation profiles ( $p > 0.05$ ) (not shown). In all cases of NEM-evoked activation, there was an initial delay in activation initiation (time to threshold), likely due to the time taken for the initial electrophile modification of TRPA1 cysteines. Importantly, there was no difference in the time to threshold between partial and full activation profiles ( $p > 0.05$ ) (Fig. 3O). In addition, there was no correlation between the time to threshold and the  $\Delta$  time to full activation (for full activations) (Fig. 3P).

Our  $\text{Ca}^{2+}$  imaging studies suggest that C665 contributes to NEM-evoked TRPA1 activation. In cell-attached recordings, we noted that NEM-evoked increases in NPo were delayed in C665S channels compared to WT (Fig. 3Q), while open channel amplitudes were no different ( $p > 0.05$ ) (Fig. 3R). A major cause of C665S's effect on NPo was the significant reduction in the percentage of channels progressing to full activation ( $p < 0.05$ ) (Fig. 3S). Importantly, there was no difference in the time to threshold between WT and C665S channels ( $p > 0.05$ ) (Fig. 3T). These data suggest that C665 is involved with the NEM-evoked progression into the full activation state, but not in the initiation of TRPA1 activation. There were few significant differences between the dwell time exponents in the P2 phase of C665S compared to WT (Fig. 3U-X): like WT, the P2 phase of C665S channels only had 3 open time exponents. Nevertheless, C665S P2 phase occupied the longest closed time exponential (Exp<sub>4</sub>) for longer than WT (Fig. 3X), and this likely contributed to the significantly reduced mean NPo for the P2 phase of C665S (Fig. 3Y).

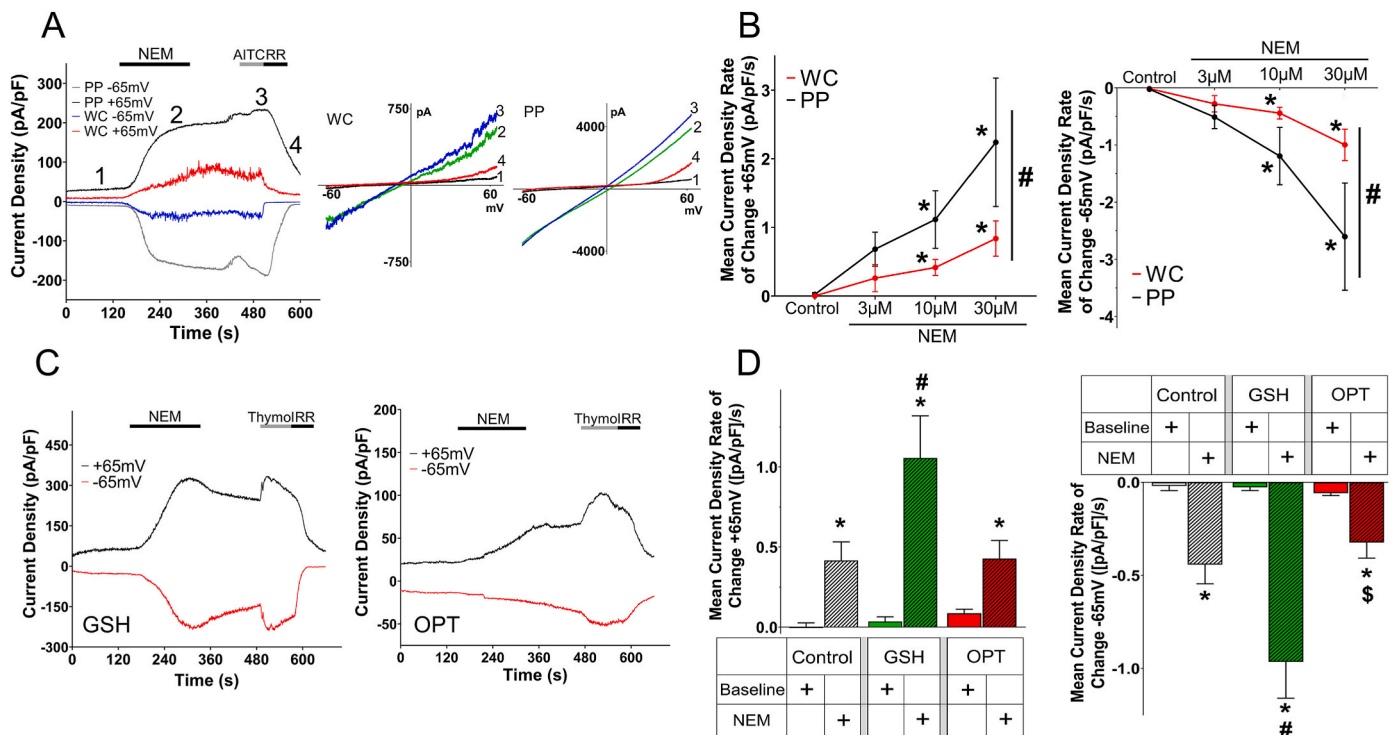


**Fig. 2.** Decreased NEM-evoked TRPA1-mediated whole-cell currents are rescued by pipette GSH. A, representative current density (+65 mV and -65 mV) and I-V graphs of TRPA1 activation in whole-cell (WC) and gramicidin-perforated patch clamp (PP) recordings during control (1), 10 μM NEM (2), 30 μM AITC (3), and 30 μM RR (4). B, mean ± S.E.M. rate of change of TRPA1-mediated currents in WC and PP during control (WC, n = 21; PP, n = 19), 3 μM (WC, n = 4; PP, n = 7), 10 μM (WC, n = 10; PP, n = 6) and 30 μM (WC, n = 7; PP, n = 5) NEM treatment at +65 mV (left) and -65 mV (right). \*, p < 0.05 vs. control; #, p < 0.05 vs. WC. C, representative current density (+65 mV and -65 mV) of whole-cell recordings with 5 mM glutathione (GSH) or 5 mM ophthalmic acid (OPT) in the pipette solution during NEM (10 μM), Thymol (200 μM), and RR (30 μM). D, mean ± S.E.M. rate of change of 10 μM NEM-induced TRPA1-mediated currents in whole-cell recordings without 5 mM GSH (control, n = 10), with 5 mM GSH (n = 10) and with 5 mM OPT (n = 9) at +65 mV and -65 mV, respectively. \*, p < 0.05 vs baseline; #, p < 0.05 vs control + NEM; \$, p < 0.05 vs GSH + NEM.

#### 4. Discussion

We observed robust and rapid electrophile-evoked TRPA1 activation in  $\text{Ca}^{2+}$  imaging studies but only gradual activation in whole-cell patch clamp experiments, similar to other studies with irreversible electrophiles such as cinnamaldehyde and prostaglandin  $\text{J}_2$  [7,9,17,18]. Whole-cell patch causes intracellular dialysis and run-down of TRPA1 currents, which is prevented by pipette solution supplementation with polyphosphates [19]. Nevertheless, our pipettes included inorganic polyphosphates, suggesting the influence of another factor. In perforated patches (which allow electrical access without membrane disruption) NEM induced robust and rapid TRPA1 activation. It should be noted that studies of  $\text{Ca}^{2+}$  imaging, whole-cell patch and perforated patch are not direct comparisons, with notable differences in membrane potential clamping and  $[\text{Ca}^{2+}]_i$ . These confounding differences were controlled for in whole-cell recordings which showed that NEM-evoked currents were greater with pipette solution supplementation with GSH compared to its inactive analog OPT or control recordings. These data indicate that electrophile-evoked TRPA1 currents in whole-cell recordings do not reflect the normal function of the channel and caution should be applied in interpreting channel biophysics under cell-ruptured conditions. Given that TRPA1 is sensitive to oxidative stress [21,22], and that endogenous GSH prevents oxidation of cytosolic thiols [23], we hypothesize that “going whole-cell” induces oxidative stress and cysteine modification that renders the channel less sensitive to subsequent electrophile treatment. Nonetheless, GSH supplementation did not increase the time taken for NEM-evoked currents to cross a lower limit threshold, suggesting other factors (e.g. membrane potential and  $[\text{Ca}^{2+}]_i$ ) may be involved.

Previous studies have identified key cysteines in TRPA1 activation by

electrophiles [12,14], but the mechanistic link between cysteine modification and activation is currently unclear. Our previous biochemical assays indicated that electrophiles rapidly bind C621 [14], and this was confirmed in cryo-EM structures of an active TRPA1 state [15,16]. Here, our data confirm that C621 is absolutely required for TRPA1 activation by electrophiles including NEM and IA. Despite initial reports [12], C641 is neither modified rapidly by electrophiles [14], nor necessary for TRPA1 activation according to our current data and another recent study [16]. Electrophiles also bind C665, although this occurs less rapidly than C621 modification [14,16]. Here, we found that C665 regulated electrophile-evoked TRPA1 activation, but this was sensitive to both the specific amino acid substitution and the electrophile. C665L mutants were completely insensitive to both NEM and IA [14,15], whereas NEM but not IA activated C665S mutants. This is consistent with other studies [15,16], and provides further evidence that larger electrophiles are capable of evoking TRPA1 activation via modification of C621 alone, whereas small electrophiles must also modify C665 for channel activation. NEM is larger than IA but smaller than the electrophile JT010, and here C665S responses were partially reduced compared to WT. It is possible that the C665L mutant prevented the conformational change evoked by C621 modification that regulates the A-loop and the downstream gating mechanism [16].

Our single-channel recordings with the irreversible electrophile NEM identified distinct TRPA1 activation phases: partial activation that for some channels was followed by a sudden switch to full activation, which (when channel inactivation is minimized) was irreversible. The channel conductance of these phases was not different, indicating no change in pore diameter. There was some variation in TRPA1 conductance across patches, likely due to the effect of variable resting membrane potential of HEK293 [29] on cell-attached patch voltage during the +40 mV step

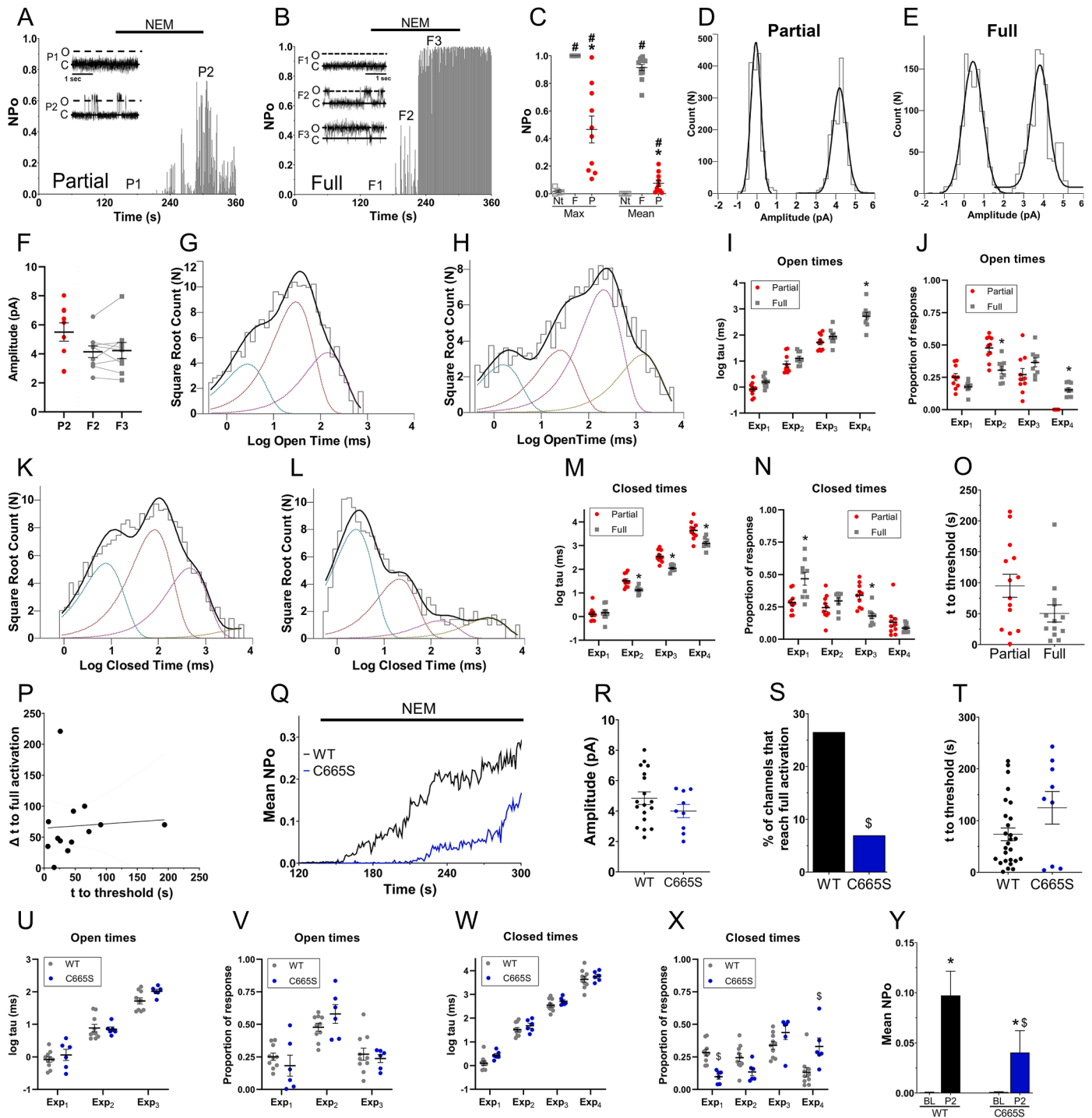


**Fig. 3.** NEM induces distinct TRPA1 activation phases in cell-attached single-channel recordings. A and B, Representative open probability (NPo) analysis of single TRPA1 channels induced by NEM (30  $\mu$ M) into partial (A) and full (B) activation phases. P1/F1 denotes prior to activation, P2/F2 denotes phase following initiation of activation, F3 denotes full activation phase. C, maximum and mean NPo analysis for full (F,  $n = 13$ ) and partial (P,  $n = 10$ ) TRPA1 activation recordings and non-transfected HEK293 (Nt,  $n = 5$ ). #,  $p < 0.05$  vs non-transfected; \*,  $p < 0.05$  vs full. D and E, amplitude histograms for partial (D) and full (E) activation shown in A and B. F, mean  $\pm$  S.E.M. current for channels induced into partial and full (separated into paired F2 and F3 phases) activation. G and H, histogram of open time distribution for partial (G) and full (H) activation shown in A and B; fitted by the sum of exponentials. I and J, mean  $\pm$  S.E.M. of open time exponential  $\tau$  (I) and proportion (J) for partial and full activation channels. \*,  $p < 0.05$  vs partial. K and L, histogram of closed time distribution for partial (K) and full (L) activation shown in A and B; fitted by the sum of exponentials. M and N, mean  $\pm$  S.E.M. of closed time exponential  $\tau$  (M) and proportion (N) for partial and full activation channels. \*,  $p < 0.05$  vs partial. O, mean  $\pm$  S.E.M. time to threshold for partial and full activation. P, Linear regression comparing the time to threshold vs.  $\Delta$  time to full activation ( $p > 0.05$ ). Q, mean NPo for all WT ( $n = 31$ ) and C665S ( $n = 19$ ) recordings during NEM treatment (30  $\mu$ M). R, mean  $\pm$  S.E.M. current for WT and C665S channels. S, percentage of TRPA1 channels that reach full activation for WT (13/49) and C665S (3/44) (\$,  $p < 0.05$ ). T, mean  $\pm$  S.E.M. time to threshold for all individually-recorded WT ( $n = 23$ ) and C665S ( $n = 12$ ) channels. U-X, mean  $\pm$  S.E.M. of open (U, V) and closed time (W, X) exponential  $\tau$  (U, W) and proportion (V, X) for partial activation (P2) in WT and C665S channels. \$,  $p < 0.05$  vs WT. Y, mean NPo analysis for partial activation (P2) in WT and C665S channels. \*,  $p < 0.05$  vs baseline (paired); \$,  $p < 0.05$  vs WT (unpaired).

[30,31]. Consistent with sequential modification of cysteines with different reactivities [14], we present three lines of evidence that the partial and ‘irreversible’ full activation phases represent distinct and potentially sequential TRPA1 activation states. Firstly, analysis of WT open times indicated that the full activation profile had the same 3 exponents as the partial profile with an additional large  $\tau$  exponent. The time spent in this fourth exponential was grossly responsible for the dramatic increase in open probability in full activation profiles. The identification of multiple exponentials suggests that TRPA1 has multiple activation states, consistent with other studies of TRP channels [32–34]. Secondly, the times taken for NEM to initiate threshold activation and to then induce full activation in WT channels were not correlated. Lastly, while there was no effect of C665S mutation on channel conductance or the time taken for NEM-evoked initiation of activation, this mutation significantly decreased the percentage of channels that reached full activation. It is likely that C665S does not affect the initial NEM-evoked activation states but rather selectively inhibits the state/states associated with higher open probability and longer open times. Importantly, the C665S mutation had little effect on TRPA1 activation by non-electrophiles, and this lack of global channel inhibition is consistent with other studies [15].

We are currently unable to model NEM-evoked TRPA1 activation, principally due to a lack of understanding of the individual contributions of each subunit in the homotetramer [24,25]. Nevertheless, we conclude that the initial activation is C665-independent and is likely due to electrophilic modification of C621, and that the time taken for NEM-treated channels to proceed into full activation depends on C665 (but it is not essential). This suggests C665 modification increases the probability for NEM-treated channels of undergoing the irreversible switch to the full state. How many activation states exist, and how many are sensitive to mutation of C665 is unclear. How these states relate to the position and stability of the A-loop [16] is also unknown.

#### Declaration of competing interest

The authors declare that they have no known competing financial interests or personal relationships that could have appeared to influence the work reported in this paper.

#### Acknowledgements

The authors wish to thank Dr. David Julius (UCSF) for the hTRPA1 plasmid and Dr. Alasdair Gibb (UCL) for discussions on single-channel analysis. This work was supported by the National Heart Lung and Blood Institute (R01HL119802 and R01HL119802-S1).

#### References

- [1] G.M. Story, A.M. Peier, A.J. Reeve, S.R. Eid, J. Mosbacher, T.R. Hricik, T.J. Earley, A.C. Hergarden, D.A. Andersson, S.W. Hwang, P. McIntyre, T. Jegla, S. Bevan, A. Patapoutian, ANKTM1, a TRP-like channel expressed in nociceptive neurons, is activated by cold temperatures, *Cell* 112 (2003) 819–829.
- [2] D.M. Bautista, S.E. Jordt, T. Nikai, P.R. Tsuruda, A.J. Read, J. Poblete, E. N. Yamoah, A.I. Basbaum, D. Julius, TRPA1 mediates the inflammatory actions of environmental irritants and proalgesic agents, *Cell* 124 (2006) 1269–1282.
- [3] C.R. McNamara, J. Mandel-Brehm, D.M. Bautista, J. Siemens, K.L. Deranian, M. Zhao, N.J. Hayward, J.A. Chong, D. Julius, M.M. Moran, C.M. Fanger, TRPA1 mediates formalin-induced pain, *Proc. Natl. Acad. Sci. U. S. A.* 104 (2007) 13525–13530.
- [4] A.N. Akopian, N.B. Ruparel, A. Patwardhan, K.M. Hargreaves, Cannabinoids desensitize capsaicin and mustard oil responses in sensory neurons via TRPA1 activation, *J. Neurosci.: Off. J. Soc. Neurosci.* 28 (2008) 1064–1075.
- [5] E. André, B. Campi, S. Materazzi, M. Trevisani, S. Amadesi, D. Massi, C. Creminon, N. Vaksman, R. Nassini, M. Civelli, P.G. Baraldi, D.P. Poole, N.W. Bunnett, P. Geppetti, R. Patacchini, Cigarette smoke-induced neurogenic inflammation is mediated by  $\alpha$ ,  $\beta$ -unsaturated aldehydes and the TRPA1 receptor in rodents, *J. Clin. Invest.* 118 (2008) 2574–2582.
- [6] A.I. Caceres, M. Brackmann, M.D. Elia, B.F. Bessac, D. Del Camino, M. D’Amours, J. A.S. Witek, C.M. Fanger, J.A. Chong, N.J. Hayward, R.J. Homer, L. Cohn, X. Huang, M.M. Moran, S.E. Jordt, A sensory neuronal ion channel essential for airway inflammation and hyperreactivity in asthma, *Proc. Natl. Acad. Sci. U.S.A.* 106 (2009) 9099–9104.
- [7] M. Bandell, G.M. Story, S.W. Hwang, V. Viswanath, S.R. Eid, M.J. Petrus, T. J. Earley, A. Patapoutian, Noxious cold ion channel TRPA1 is activated by pungent compounds and bradykinin, *Neuron* 41 (2004) 849–857.
- [8] S.-E. Jordt, D.M. Bautista, H. Chuang, D.D. McKemy, P.M. Zygmunt, E.D. Högestätt, I.D. Meng, D. Julius, Mustard oils and cannabinoids excite sensory nerve fibres through the TRP channel ANKTM1, *Nature* 427 (2004) 260–265.
- [9] T.E. Taylor-Clark, B.J. Undem, D.W. Macglashan Jr., S. Ghatta, M.J. Carr, M. A. McAlexander, Prostaglandin-induced activation of nociceptive neurons via direct interaction with transient receptor potential A1 (TRPA1), *Mol. Pharmacol.* 73 (2008) 274–281.
- [10] T.E. Taylor-Clark, M.A. McAlexander, C. Nassenstein, S.A. Sheardown, S. Wilson, J. Thornton, M.J. Carr, B.J. Undem, Relative contributions of TRPA1 and TRPV1 channels in the activation of vagal bronchopulmonary C-fibres by the endogenous autacoid 4-oxononenal, *J. Physiol.* 586 (2008) 3447–3459.
- [11] T.E. Taylor-Clark, F. Kiros, M.J. Carr, M.A. McAlexander, Transient receptor potential ankyrin 1 mediates toluene diisocyanate-evoked respiratory irritation, *Am. J. Respir. Cell Mol. Biol.* 40 (2009) 756–762.
- [12] A. Hinman, H.H. Chuang, D.M. Bautista, D. Julius, TRP channel activation by reversible covalent modification, *Proc. Natl. Acad. Sci. U. S. A.* 103 (2006) 19564–19568.
- [13] L.J. Macpherson, A.E. Dubin, M.J. Evans, F. Marr, P.G. Schultz, B.F. Cravatt, A. Patapoutian, Noxious compounds activate TRPA1 ion channels through covalent modification of cysteines, *Nature* 445 (2007) 541–545.
- [14] P.K. Bahia, T.A. Parks, K.R. Stanford, D.A. Mitchell, S. Varma, S.M. Stevens, T. E. Taylor-Clark, The exceptionally high reactivity of Cys 621 is critical for electrophilic activation of the sensory nerve ion channel TRPA1, *J. Gen. Physiol.* 147 (2016) 451–465.
- [15] Y. Suo, Z. Wang, L. Zubcevic, A.L. Hsu, Q. He, M.J. Borgnia, R.R. Ji, S.Y. Lee, Structural insights into electrophile irritant sensing by the human TRPA1 channel, *Neuron* 105 (2020) 882–894, e5.
- [16] J. Zhao, J.V. Lin King, C.E. Paulsen, Y. Cheng, D. Julius, Irritant-evoked activation and calcium modulation of the TRPA1 receptor, *Nature* 585 (7823) (2020) 141–145.
- [17] T.E. Taylor-Clark, S. Ghatta, W. Bettner, B.J. Undem, Nitrooleic acid, an endogenous product of nitrate stress, activates nociceptive sensory nerves via the direct activation of TRPA1, *Mol. Pharmacol.* 75 (2009) 820–829.
- [18] A. Hynkova, L. Marsakova, J. Vaskova, V. Vlachova, N-terminal tetrapeptide T/SPLH motifs contribute to multimodal activation of human TRPA1 channel, *Sci. Rep.* 6 (2016) 28700.
- [19] D. Kim, E.J. Cavanaugh, Requirement of a soluble intracellular factor for activation of transient receptor potential A1 by pungent chemicals: role of inorganic polyphosphates, *J. Neurosci.* 27 (2007) 6500–6509.
- [20] D.A. Andersson, C. Gentry, S. Moss, S. Bevan, Transient receptor potential A1 is a sensory receptor for multiple products of oxidative stress, *J. Neurosci.: Off. J. Soc. Neurosci.* 28 (2008) 2485–2494.
- [21] N. Takahashi, Y. Mizuno, D. Kozai, S. Yamamoto, S. Kiyonaka, T. Shibata, K. Uchida, Y. Mori, Molecular characterization of TRPA1 channel activation by cysteine-reactive inflammatory mediators, *Channels* 2 (2008) 287–298.
- [22] J.H. Keen, W.B. Jakoby, Glutathione transferases. Catalysis of nucleophilic reactions of glutathione, *J. Biol. Chem.* 253 (1978) 5654–5657.
- [23] M.J.M. Fischer, D. Balasuriya, P. Jeggel, T.A. Goetze, P.A. McNaughton, P.W. Reeh, J.M. Edvardson, A. Hazan, R. Kumar, H. Matzner, A. Priel, K. Hill, M. Schaefer, Y. Sawada, H. Hosokawa, K. Matsumura, S. Kobayashi, Direct evidence for functional TRPV1/TRPA1 heteromers, *Eur. J. Neurosci.* 466 (2014) 7145–7153.
- [24] W. Ye, Y.-H. Tu, A.J. Cooper, Z. Zhang, Y. Katritch, E.R. Liman, Activation stoichiometry and pore architecture of TRPA1 probed with channel concatemers, *Sci. Rep.* 8 (2018) 17104.
- [25] Y.Y. Wang, R.B. Chang, H.N. Waters, David D. McKemy, E.R. Liman, The nociceptor ion channel TRPA1 is potentiated and inactivated by permeating calcium ions, *J. Biol. Chem.* 283 (2008) 32691–32703.
- [26] D. Colquhoun, F.J. Sigworth, Fitting and statistical analysis of single-channel records, in: *Single-Channel Recording*, 1995, pp. 483–587.
- [27] F.J. Sigworth, S.M. Sine, Data transformations for improved display and fitting of single-channel dwell time histograms, *Biophys. J.* 52 (1987) 1047–1054.
- [28] J. Chemin, A. Monteil, C. Briquaire, S. Richard, E. Perez-Reyes, J. Nargeot, P. Lory, Overexpression of T-type calcium channels in HEK-293 cells increases intracellular calcium without affecting cellular proliferation, *FEBS Lett.* 478 (2000) 166–172.
- [29] R. Fischmeister, R.K. Ayer, R.L. DeHaan, Some limitations of the cell-attached patch clamp technique: a two-electrode analysis, *Pflügers Arch. Eur. J. Physiol.* 406 (1986) 73–82.
- [30] K.L. Perkins, Cell-attached voltage-clamp and current-clamp recording and stimulation techniques in brain slices, *J. Neurosci. Methods* 154 (2006) 1–18.
- [31] J. Benedikt, A. Samad, R. Ettrich, J. Teisinger, V. Vlachova, Essential role for the putative S6 inner pore region in the activation gating of the human TRPA1 channel, *Biochim. Biophys. Acta Mol. Cell Res.* 1793 (2009) 1279–1288.
- [32] J.A. Canul-Sánchez, I. Hernández-Araiza, E. Hernández-García, I. Llorente, S. L. Morales-Lázaro, L.D. Islas, T. Rosenbaum, Different agonists induce distinct single-channel conductance states in TRPV1 channels, *J. Gen. Physiol.* 150 (2018) 1735–1746.
- [33] K. Hui, B. Liu, F. Qin, Capsaicin activation of the pain receptor, VR1: multiple open states from both partial and full binding, *Biophys. J.* 84 (2003) 2957–2968.